Available online at www.sciencedirect.com
ScienceDirect
Pattern Recognition 40 (2007) 189–197
PATTERN RECOGNITION
THE JOURNAL OF THE PATTERN RECOGNITION SOCIETY
www.elsevier.com/locate/patcog

Fingerprint matching from minutiae texture maps

F. Benhammadi*, M.N. Amirouche, H. Hentous, K. Bey Beghdad, M. Aissani

Laboratory of Computer Science, M. P. School BP, 17, Bordj-El-Bahri 16111 Algiers, Algeria

Received 21 January 2006; received in revised form 31 May 2006; accepted 24 June 2006

Abstract

The fingerprint matching using the original FingerCode generation has proved its effectiveness but it suffers from some limitations such as the reference point localization and the recourse to the relative fingerprint pre-alignment stage. In this paper, we propose a new hybrid fingerprint matching technique based on minutiae texture maps according to their orientations. Therefore, rather than exploiting the eight fixed directions of Gabor filters for all original fingerprint images filtering process, we construct absolute images starting from the minutiae localizations and orientations to generate our weighting oriented Minutiae Codes. The extracted features are invariant to translation and rotation, which allows us avoiding the fingerprint pair relative alignment stage. Results are presented demonstrating significant improvements in fingerprint matching accuracy through public fingerprint databases.

Keywords: Minutiae texture matching; Hybrid fingerprint matching; Gabor filter

1. Introduction

Biometric are automated methods of recognizing a person based on his/her physical or behavioral characteristics. Nowadays, many commercial applications use fingerprint, face, iris, hand geometry, voice and dynamic signature. The fingerprint technique is the most solicited; therefore, several fingerprint matching approaches have been proposed in the last years. These approaches differ with respect to the fingerprint features used for matching. We can distinguish three categories: minutiae-based matching [1–3], correlation-based matching [4,5] and texture-based matching [6–10]. The first category is used widely; but recently, the two others are receiving considerable interest since their hybridization with the first category seems to be a promising way to improve the fingerprint matching for identification and verification systems accuracy [11].

The fingerprint matching proposed in Ref. [6] describes fingerprints through their macro-features. This approach uses the circular tessellation of the filtered images centered at a reference point to generate eight-dimensional features maps and computes their average absolute deviation (AAD) features (FingerCodes). Hence, the authors use some FingerCodes as feature maps (templates) for a possible matching in case the fingerprint is oriented up to $\pm 45°$. Obviously, the matching performance of this method is directly proportional to the localization of reference point and to the quality of the fingerprint images. Moreover, the authors specified that their method cannot guarantee that a reference point will be found on every type of fingerprint image such as the arch-type and for the poor quality fingerprint images.

Several attempts have been made to improve fingerprints alignment and the localization reference point. The approach proposed by Ross et al. [11], where the fingerprint alignment exploits the spatial coordinates of the reference minutiae pair, resulted in the best alignment of the template and input fingerprint images. Other approaches were proposed in Refs. [7,12] to generate a unique reference point for robust localization. However, these methods used the rotation-invariant reference point location and combined the direction features in order to improve the overall matching performance. Other authors have used the generalized Hough transform (GHT) for point pattern matching [13,14].

* Corresponding author. Tel.: +213 21863469; fax: +213 21863204.
E-mail addresses: benhammadif@yahoo.fr (F. Benhammadi), amirouchenab@yahoo.fr (M.N. Amirouche),hentoush@yahoo.fr (H. Hentous), bey_kadda@yahoo.fr (K. Bey Beghdad), maissanim@yahoo.fr (M. Aissani).

0031-3203/$30.00
doi:10.1016/j.patcog.2006.06.031

The fingerprint alignment problem still persists because the preceding approaches do not avoid the relative pre-alignment stage to recover the geometric transformation (generally translation and rotation) between the template and the input fingerprint. So, this stage remains a difficult task, especially when the database contains a large amount of minutiae features extraction errors. To avoid the relative pre-alignment, some authors perform minutiae matching locally [15,16]. Others propose to try to match minutiae globally [17]. They introduce an intrinsic coordinate system based on portioned regular regions defined by the orientation field and the minutiae are defined with respect to their position in this coordinate system. This approach has some practical problems such as reliably partitioning the fingerprint in regular regions and unambiguously defining intrinsic coordinate axes in poor quality fingerprint images [18].

In order to overcome the problems of this relative pre-alignment stage, we propose a new fingerprint matching approach from invariant texture features which produces the matching method with the absolute pre-alignment obtained from the minutiae features. In other words, we characterize each fingerprint by a FingerCode which is generated with respect to individual minutiae according to minutia localization and orientation rather than exploiting the reference point as the original approach. Additionally, we reinforce these feature vectors by weighting the AAD features of sectors according to the presence of minutiae in these sectors in order to have a hybrid fingerprint matching. Thus, this manner of generation produces the invariant FingerCode to the geometric transformations and avoids the relative fingerprint pre-alignment stage. Results are presented demonstrating significant improvements in fingerprint matching accuracy through the fingerprint databases. In addition, our approach is able to deal with partial fingerprint, where sometimes, reference point cannot be reliably detected, or it is close to the border in poor quality image.

This paper is organized as follows: Section 2 introduces the oriented minutiae codes which are exploited in Section 3 for our texture-based fingerprint matching algorithm. Finally, Section 4 presents the performance and limits of our matching approach.

2. Minutiae texture maps

There are two basic types of minutiae extraction methods which exploit the binarized or the gray-scale fingerprint images. The first technique transforms the gray level fingerprint images into binary images on which a thinning process is applied [2]. The minutiae are then extracted from the thinned fingerprint images. The other method exploits the direct gray-scale images extraction which is more efficient than the first one [19]. For feature vector extraction, we use the filter-bank-based as compact fixed length feature vector (FingerCode) introduced in the original approach [6].

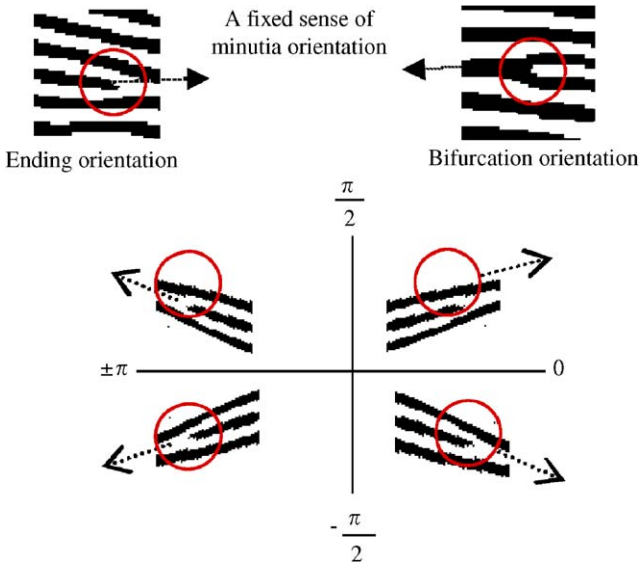

Fig. 1. The convention ridge orientation.

But, our generation utilizes the localization and the direction information that characterizes the oriented flow pattern of each detected minutia in the two stages: reference point localization and its oriented FingerCode generation starting from the minutia orientation.

2.1. Convention minutiae orientation

Thus, for each detected minutia, the following parameters are recorded:

1. x and y coordinate of the minutia point.
2. θ the minutia orientation which is defined as the local ridge-valley direction.

Although the ridge-valley orientation values have the range $\left[-\frac{\pi}{2}, \frac{\pi}{2}\right]$ in the classical orientation estimate,[1] the minutia in our method must be redirected into the range $[-\pi, \pi]$ to increase its discrimination. For that, we associate the ridge orientation with their types (i.e. ends abruptly and converges bifurcation). For this reason, we defined a convention as shown in Fig. 1. Using this convention, we can say that two ending ridges of opposite directions θ and $\theta + \pi$ are not both along a line of orientation θ if the fixed sense ridge-valley orientations are opposite. Thus, in our approach, the ridge-valley orientation values have the range $[-\pi, \pi]$.

2.2. Interest minutiae zone determination

In our approach, the reference point is usually selected as the minutia point extracted from fingerprint. Each minutia texture map represents the original Fingercode. Therefore,

[1] We have chosen to implement the method introduced in Ref. [20].

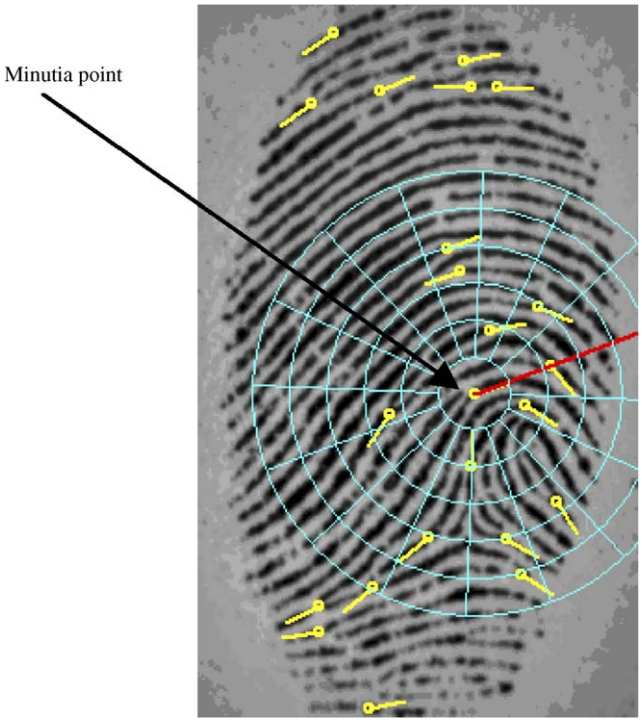

Fig. 2. The interest minutia zone.

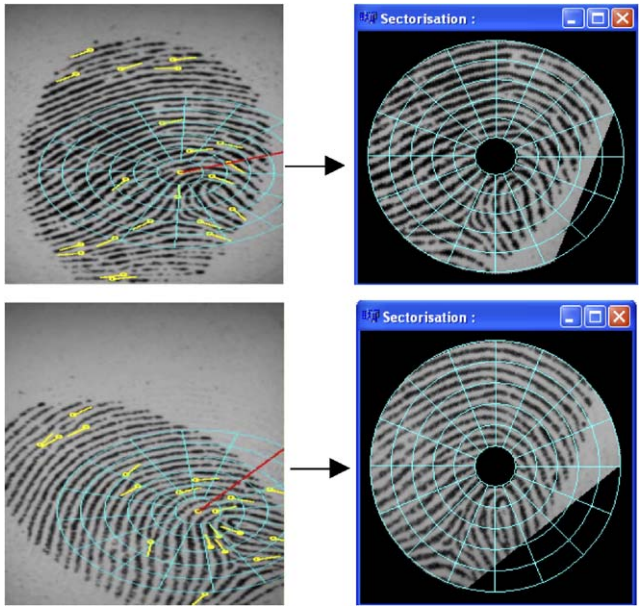

Fig. 3. The invariant IMZ to the geometric transformation.

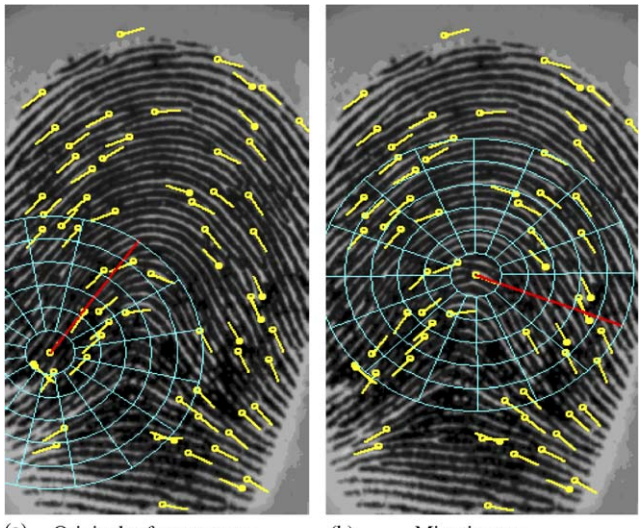

Fig. 4. Reference point location: (a) Original reference core, (b) minutia core.

the tessellation generation can be summarized in the following steps:

1. Determination of the region of interest for the local fingerprint image surrounding each minutia. This region, called *interest minutia* zone (IMZ), contains a number of fingerprint features (minutiae) (Fig. 2).
2. Tessellation of the interest minutia zone. This subregion is determined by a circular tessellation using 80-dimentional vector ($16 * 5$ sectors: S_0 through S_{79}) used in the original approach [6]. But our tessellation is invariant to the geometric transformations and avoids the fingerprint relative pre-alignment stage as shown in Fig. 3. The original reference point method is, therefore, not very robust with respect to errors in the location of this point as illustrated for the same fingerprint images in Fig. 4.
3. Normalization of the interest minutia zone. This step normalizes the gray level intensities using constant mean M_0 and variance V_0 separately for each sector to remove the noise effects due to the sensor fingerprint capture. Thus, we adopt the same values as in the original approach [6] using both M_0 and V_0 to a value of 100.

2.3. Interest minutiae zone filtering

The interest minutia zone is filtered in eight directions using a bank of Gabor filters. The only difference between our approach and the original one lies in the choice of the Gabor filters directions. The original approach uses eight fixed directions $(0°; 22.5°, 45°, 57.5°, \ldots, 157.5°)$ whereas but our approach adapts these eight directions according to the minutia orientation. In other words, the first direction of the eight Gabor filters corresponds to the minutia orientation. For example, if we have 65° for the orientation minutia, the eight directions of Gabor filter are 65°, 87.5°, 110°, 132.5°, 155°, 177.5°, 20° and 42.5°. Thus, the filtering process produces a set of eight filtered images according to each minutia orientation that characterizes each fingerprint by its own features (the minutiae orientations). The original approach uses Gabor filter that

has the following general form in the special domain:

$$G(x, y, f, \theta) = \left\{ \frac{-1}{2} \left[\frac{x'^2}{\delta_x^2} + \frac{y'^2}{\delta_y^2} \right] \right\} \cos(2\pi f x'), \quad (1)$$

$$x' = x \sin(\theta) + y \cos(\theta),$$

$$y' = x \cos(\theta) - y \sin(\theta),$$

where f is the frequency of the sinusoidal plane wave along the direction θ (also the minutia orientation) with respect to the x-axis, and $\delta_{x'}$ and $\delta_{y'}$ are the standard deviations of the Gaussian envelope along x' and y'-axis, respectively. We have chosen the same parameters values as the original approach [6] ($f = 0.1$; $\delta_{x'} = \delta_{y'} = 4.0$).

2.4. The oriented minutia code generation

After filtering the interest zone generation, we determine the oriented minutia code. Around each minutia point, five concentric circular regions of 20 pixels wide which represent the inter-ridge distances are defined and each region is divided into 16 sectors as defined in Ref. [6].

Thereafter, we generate the OMC which represents eighty features for each of the eight filtered images according to each minutia m_c orientation. This provides a total of 640 (80×8) because our approach uses a feature vector which contains the magnitude value of the original AAD from the mean of the interest minutiae zone (80 sectors). An example of OMC is shown in Fig. 6, where the disks correspond to the eight Gabor filtered images according to the minutia orientation value equal to 15°. Our OMC generation produces invariant feature vector because this generation starts from the minutia orientation while going clockwise to the other sectors. For this reason, the original collection of all the sectors S_i will be slightly modified by starting from the minutia orientation θ_{m_c} as follows:

$$S_i = \left\{ \begin{array}{l} (x, y) | b(T_i + 1) \leqslant r < b(T_i + 2), \theta_i \leqslant \theta < \theta_{i+1}, \\ 1 \leqslant x \leqslant N, \quad 1 \leqslant y \leqslant M, \end{array} \right\} \quad (2)$$

where k represents the number of sectors and the angle for each sector S_i must lie between $\theta_i = \theta_{m_c} + (i \bmod k)(2\pi/k)$ and $\theta_{i+1} = \theta_{m_c} + ((i+1) \bmod k)(2\pi/k)$ instead of $\theta_i = ((i+1) \bmod k)(2\pi/k)$ and $\theta_{i+1} = ((i+1) \bmod k)(2\pi/k)$ as defined in the original approach [6].

Thus, this manner of generation allows obtaining a feature vector which is practically invariant to geometrical transformations (rotation and translation). According to the convention (Fig. 1), each OMC remains unchanged because the generation uses absolute pre-alignment according to the minutia orientation. For example, the OMCs of the two fingerprints illustrated in Fig. 3, are shown in Fig. 5.

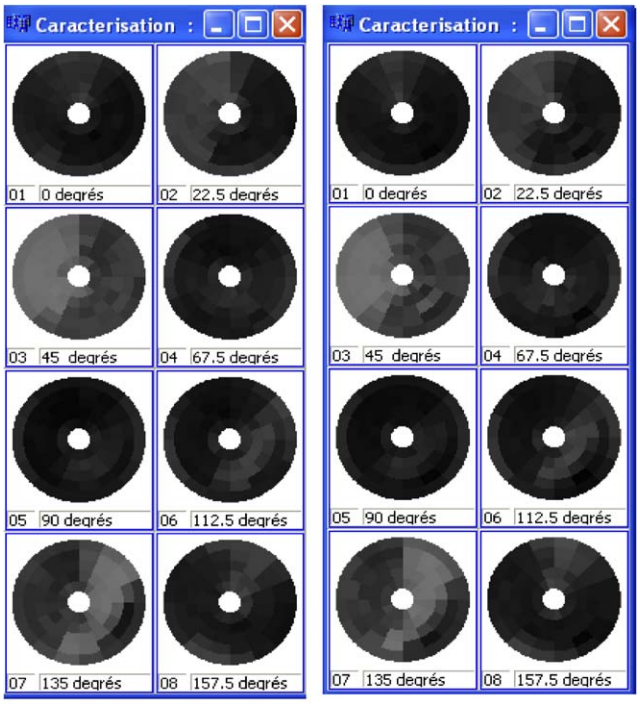

Initial image Transformed image

Fig. 5. The invariant OMCs generation.

The novelty in our approach is to assign weights to sectors containing minutiae which will permit to distinguish better two textures. This assignation consists of weighting the AAD (noted AAD_P) features of sectors according to the presence of minutiae in these sectors. In other words, the AAD of the sector that contains a minutia is multiplied by a weighting factor W in order to differentiate between sectors that contain the minutiae features and the other sectors; and those that contain a certain proportion of background pixels are labeled as background sectors and the corresponding AAD feature value is set to 0. This new technique characterizes sectors of the sectorization by minutiae localization in the fingerprint images which produces a hybrid fingerprint matcher

$$AAD_P(S_i) = \begin{cases} AAD(S_i) * W & \text{If sector contains minutia,} \\ AAD(S_i) & \text{Else,} \\ 0 & \text{Background sector.} \end{cases} \quad (3)$$

As a result, we obtain for the minutia an oriented FingerCode that describes its local and global characteristics. It contains the feature vector for each sector S_i ($i = 0, \ldots, 79$) which has the weighted average absolute derivation from the mean as defined in Ref. [6].

3. Fingerprint matching algorithm

The fingerprint matching task is more difficult and the major existing approaches do not avoid the absolute

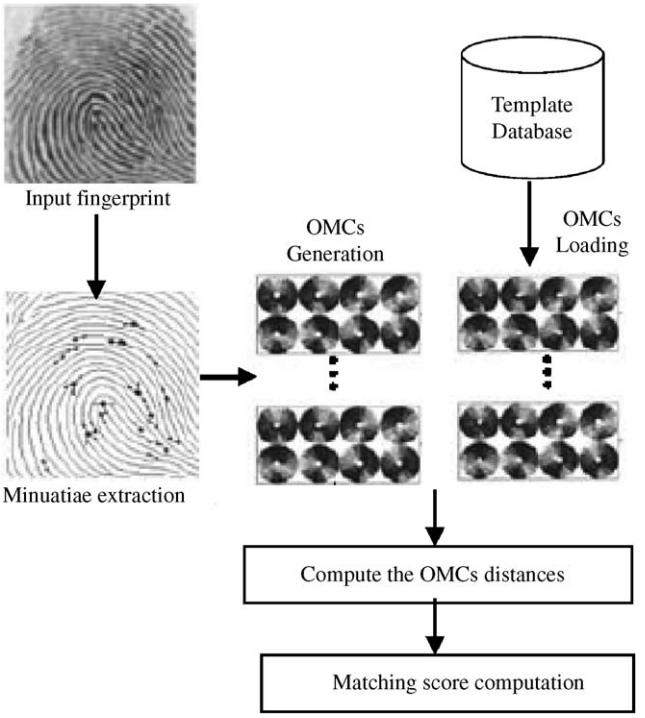

Fig. 6. The matching process.

pre-alignment of the input fingerprint and the template images. The focus of this section is to discuss our algorithm for automatic fingerprint matching which is performed by texture-based pattern matching using the proposed OMCs. When verification or identification process is necessary, the OMCs are extracted from the user's presented finger, and they are compared to the OMCs (templates) from the database, as illustrated by the flow chart in Fig. 6.

Let $T = \{m_i, i = 1 \cdots n\}$ and $I = \{m'_j, j = 1 \cdots m\}$ be the minutiae lists extracted from the template and input fingerprint, respectively.

Let $F^{\theta_i}_{m_i}(x, y)$ be the θ_i-direction filtered image for fingerprint image, where θ_i represents the minutia m_i direction. We define a feature vector for each minutia m_i according to their $F^{\theta_i}_{m_i}(x, y)$ as $V^{\theta_i}_{m_i}$. It contains the weighted magnitude value of the AAD according to the minutiae presence for any sector S_i $(i = 0, \ldots, 79)$.

The similarity of paired minutiae is based on the minimization of the distances between the OMCs. Let $V^{\theta}_{m_i}$ and $V^{\theta}_{m_j}$ denote the feature vectors of a template minutia m_i and the input minutia m_j, respectively. We define distance D_k between the component pairs k of the two feature vectors $V^{\theta}_{m_i}$ and $V^{\theta}_{m_j}$ as follows:

$$D_k(V^{\theta}_{m_i}, V^{\theta}_{m_j}) = \frac{(V^{\theta}_{m_i}(k) - V^{\theta}_{m_j}(k))^2}{\sigma^2(V^{\theta}_{m_i}) + \sigma^2(V^{\theta}_{m_j})}. \quad (4)$$

As a consequence, the resulting distance between two feature vectors $V^{\theta}_{m_i}$ and $V^{\theta}_{m_j}$ can be chosen as

$$D(V^{\theta}_{m_i}, V^{\theta}_{m_j}) = \sum_{k=0}^{k=79} D_k(V^{\theta}_{m_i}, V^{\theta}_{m_j}). \quad (5)$$

Then, the distance between the two OMCs according to the minutiae m_i and m_j is defined by the following formula:

$$D(m_i, m_j) = \sum_{k=0}^{k=7} D(V^{\theta_k}_{m_i}, V^{\theta_k}_{m_j}), \quad (6)$$

where θ_k represents the eight directions using a bank of Gabor filters.

The score matching degree will then be established by the minimization of the distances of each paired minutia m_i belonging to the template fingerprint and all minutiae m'_j for $j = 0 \ldots m$ belonging to the input fingerprint. This is defined by the following formula:

$$SM = \underset{j=0 \ldots m}{Min} (D(m_i, m'_j)). \quad (7)$$

It is very difficult, if not altogether impossible, to obtain performance from minutiae extraction task owed to the poor quality of fingerprint images. So, the minutiae location errors, caused by the orientation field estimation, generate improper OMCs. The two images (Fig. 7) show the impact of minutia localization and orientation errors on the sectors in the sectorization process construction. So, the localizations of the minutiae in the sectors are completely different in the two tessellations. This produces the different corresponding OMCs computed from these sectorizations because the AAD_P of the sectors by the weighting factor W is following the adherence of these minutiae in the sectors. Fig. 7 shows this situation of tessellation characterization well. For example, the AAD of the sector S_7 is weighted by weighting factor in the input image tessellation and the AAD of the sector S_{24} is weighted in the template image tessellation. Besides, these orientation errors essentially generate some different features for the external sectors. Otherwise, there errors produce a shift of a sector in the circular tessellation and feature vector characterization. For example, if we have an orientation error equal to $+15°$, all sectors will be shifted by one position: the sector S_0 becomes the sector S_1 and so on.

To address this problem, we propose stage consolidation. Hence, we introduce two variation techniques to ensure a good extraction of fingerprint features. Let us note that these variations do not represent the alignment of the two fingerprints but the corrections of the minutiae localization and orientation errors caused by the extraction algorithm. The first one is the minutia orientation variation of $\pm\Delta\theta°$ to correct orientation extraction errors as shown in Fig. 8. This variation allows the correction of the weighted AADs of the sectors that belong to the same concentric circular regions (same band).

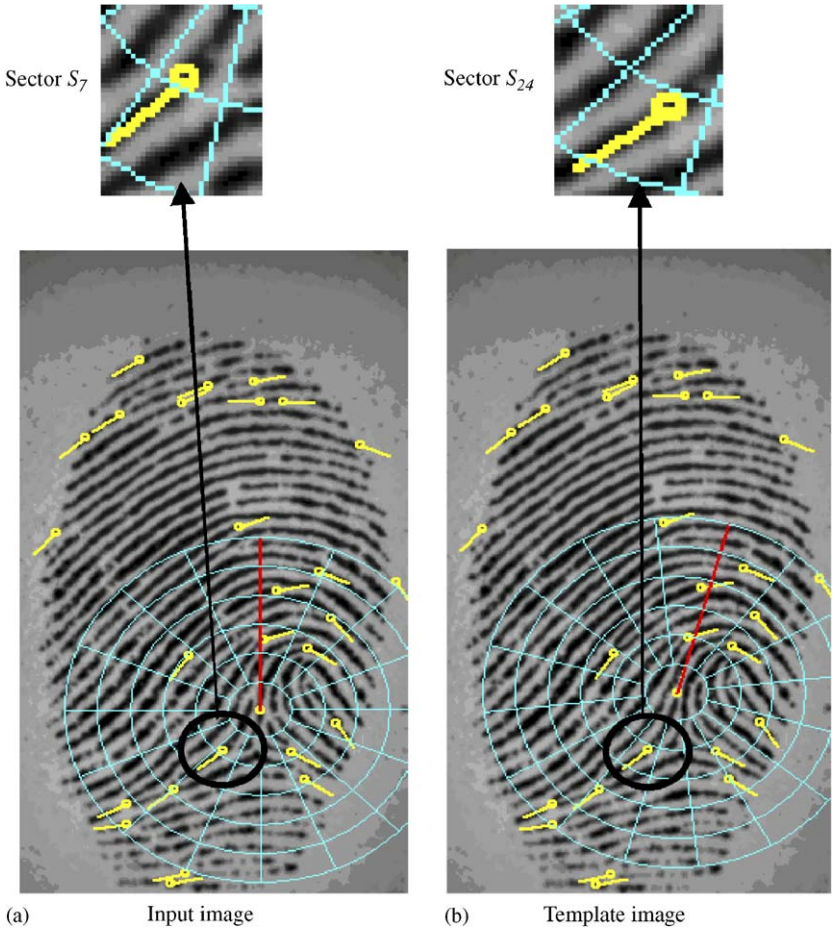

Fig. 7. The influence of minutia features extraction on the OMC generation: (a) Input image, (b) template image.

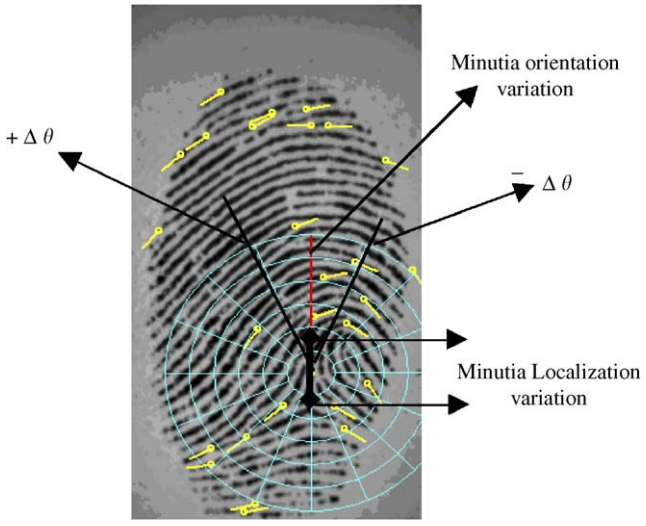

Fig. 8. The minutia variation.

The second variation is the minutia localization variation on the ridge segment of which belongs the minutia following the orientation axis. This variation has a larger effect in correcting errors on adjacent bands while positioning minutiae in the adequate sectors to compute the weighted AADs. Hence, this variation compensates the minutia localization errors compared to that introduced in Ref. [21].

In the continuation of this section, we are going to clarify these two variation techniques.

Let us reconsider the preceding input fingerprint image in Fig. 7(a). If the minutia extraction module produces 90° as a minutia orientation, we use thirty-one (31) possible orientations for variation errors in the range $[-15, +15]$ with 1° as variation step (75°, 76°, ..., 90°, ..., +104°, 105°). So, the 15th variation of the minutia orientation according to the clockwise sense (−15°) (image (a), Fig. 9) and a displacement of seven pixels in the sense of the minutia orientation give us the tessellation of template fingerprint image (image (b), Fig. 9) that corresponds to the template fingerprint image in Fig. 7(b).

Thus, for each minutia pairing from template fingerprint, we need various OMCs computed from some filtered Gabor images. Finally, these variations manage the minutia extraction errors for the weighted AAD of the set of sectors located in the bands of the interest minutia zone during the feature vector generation.

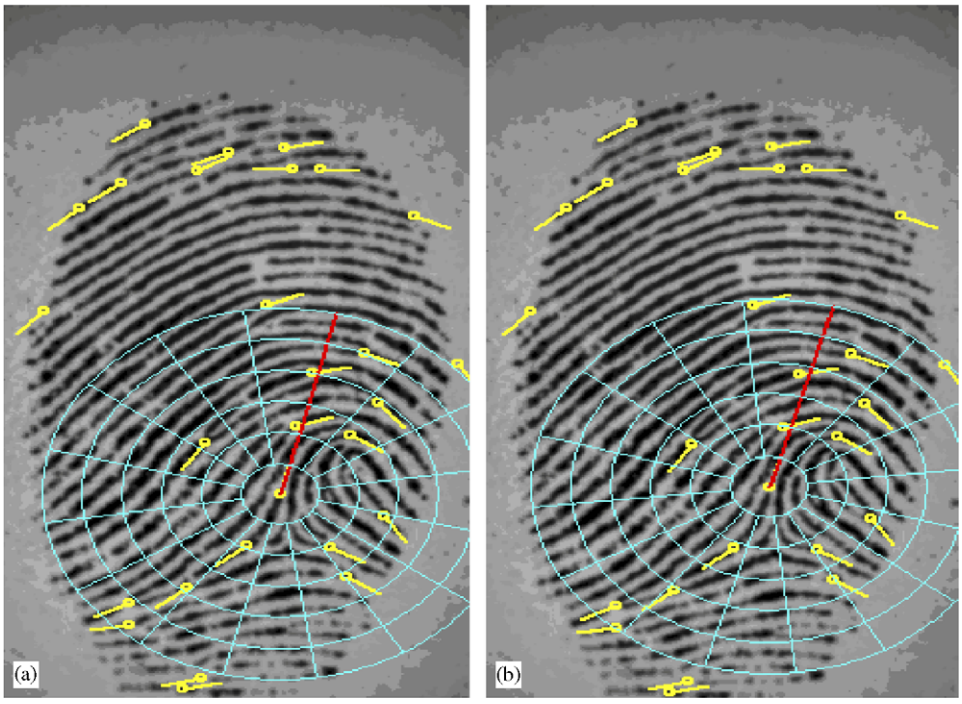

Fig. 9. The minutia localization and orientation correction.

Table 1
EERs estimated on DB1 FVC2000 for different orientation variations

$\Delta\theta$	0°	±1°	±2°	±3°	±7°	±9°
DB1	7.1	6.73	6.39	6.21	6.01	5.99

4. Experimental results

In order to confirm the effectiveness of our proposed fingerprint texture-based matching approach, we carried out experiments of the minutiae textures verification. Conditions of the experiments are as follows. All experiments discussed in this paper are conducted on a Pentium IV 3.6 GHz and exploit the DB1 and all databases from fingerprint databases used in the Fingerprint Verification Competition FVC2000 and FVC2002 [18], respectively. So, each base contains 100 distinct fingers and each finger has eight impressions ($8*100$). During our experiments, we have used three bands solely for tests (48 sectors).

To expose the impact of the minutiae orientation variations on the accuracy of fingerprint matching, we varied the minutiae orientations and computed the corresponding false accept rates (FAR), false reject rates (FRR) and their corresponding equal error rates (EER) are plotted in Fig. 10 only for the DB1 FVC2000 with orientation minutia variation $\Delta\theta = \pm 9°$. So, the use of the variation errors produces more effective results. The results in Table 1 show that the use of a large range of minutia orientation errors caused by the extraction module yield an EER less than 6%. Fig. 11 graphically illustrates the genuine and imposter distributions in this case (an orientation variation $\Delta\theta = \pm 9°$).

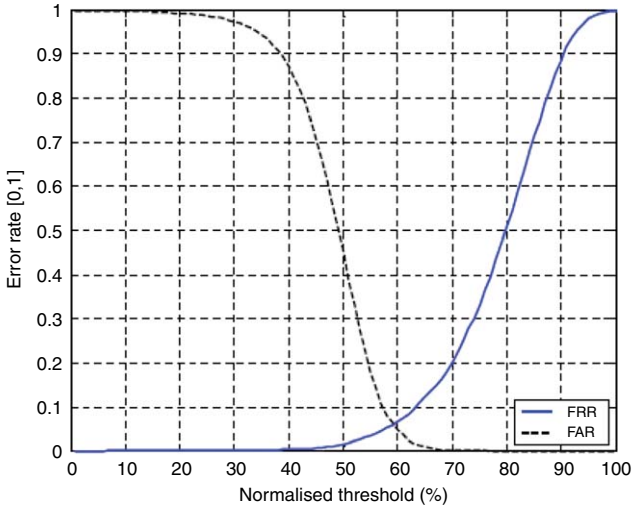

Fig. 10. EER-curve on DB1 FVC2000 obtained with $\Delta\theta = \pm 9°$.

During the experiments, we have observed that the EER increase from a minutia orientation variation of 10°. It means that our minutia extraction module produces orientation errors close to 10°. Besides, the effectiveness of our method decreases with an incorrect minutia localization which is caused by the minutiae extraction module (Approximately 11% of extraction errors between the missing and false minutiae), in particular the last one that entails an incorrect tessellation for the matching process. Fig. 12 shows the comparison of the corresponding EER with different number of matching minutiae orientation variations (0°, 5° and 9°).

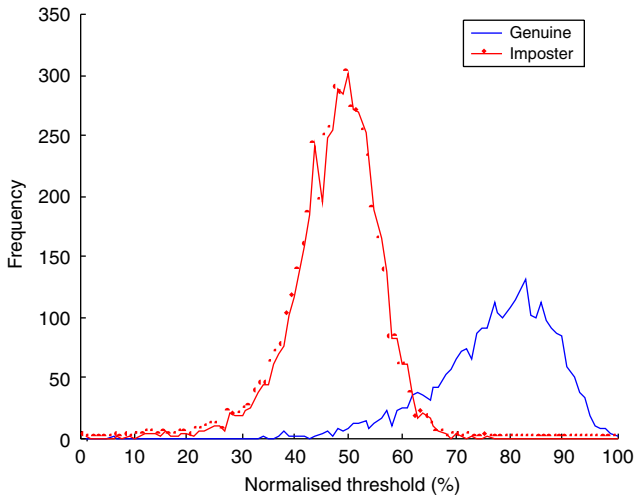

Fig. 11. Genuine and imposter distributions on DB1FVC200 obtained with $\Delta\theta = \pm 9°$.

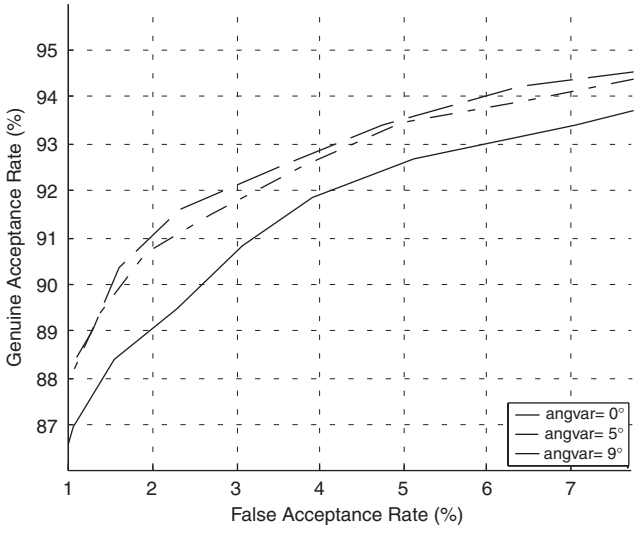

Fig. 12. ROC curves on DB1 FVC2000 with different orientation variations (0°, 5° and 9°).

Table 2
Average results over all databases FVC2002

	DB1-a	DB2-a	DB3-a	DB4-a	All databases
EER (%)	4.27	2.61	10.63	5.12	5.19
Average enrollment time (s)	5.36	4.71	5.94	5.04	5.31
Average matching time (s)	3.15	2.02	3.01	2.87	2.42

The matching performances achieved on all fingerprint databases FVC2002 are shown in Table 2 with minutia localization errors in the range ±7 pixels (two pixels as variation step) and $\Delta\theta = \pm 9°$ as orientation variations.

Obviously, the experiments conducted over a sample of all fingerprint image bases indicate that the improving matching accuracy is directly proportional to the minutiae orientation range.

Table 3
Ranking of our approach on all databases of the Top 31 participants in FVC2002

	DB1-a	DB2-a	DB3-a	DB4-a	All databases
Rank	22	16	23	19	17

On the other hand, our approach consumes more time in the enrollment and the matching process. It is due to the OMCs generation phase of all minutiae belonging to the input fingerprint images. However, each fingerprint template in the databases is pre-aligned, independently of the others and stored as the feature vectors. So, each template fingerprint in the database is represented by the oriented minutiae codes that represent all minutiae belonging.

We will present in Table 3, the rank of our approach compared to the results obtained by the different algorithms presented to the FVC2002 competition from the same bases (according to the EER) [22].

We note that an EER of 5.19% is quite acceptable in comparison with those of the results in Ref. [22]. So, our matching algorithm is ranked according to the EER in the 13th, the fourth and in the second position in relation to all algorithms coming from industry, others and academies, respectively.

As comparison to the original approach [6], we give here errors of the reference point localization and ERR reported in Ref. [23]. Therefore, to evaluate the found original reference points on all databases FVC2002, their locations are further computed by an original method. The results show that 11.75%, 9.25%, 21.62% and 14.27% of the reference points were not correctly located (Fail to enroll) on DB1-a, DB2-a, DB3-a and BD4-a, respectively. The remaining error cases are due to the noise or to the fact that the reference point is close to the border in poor quality images or to scars near the reference points in particular DB3-a. Moreover, the ERR for all databases FVC2002 are 12.5%, 11.7%, 29% and 18% as reported in Ref. [23], respectively. Then, our matching algorithm allows us obtaining improvements in comparison to the original approach. Moreover, this method is more effective compared to the one introduced in Ref. [21] because it deals with the localization variation.

5. Conclusion

The conducted testing of a novel fingerprint matching technique using the minutiae texture maps shows good correspondence to the fingerprint identification. Our matching algorithm avoids the use of the relative pre-alignment because we take advantage of the oriented minutiae codes that are invariant to the geometric transformations. The usefulness of this approach was confirmed in the experiments

conducted here, which reveals that the identification results are encouraging and our approach is promising. We project to overcome the strong local or global deformations and to propose a distributed matching algorithm for the minutiae texture maps extraction to improve the computation times of our matching approach.

References

[1] M. Tico, P. Kuosmanen, Fingerprint matching using an orientation-based minutia descriptor, IEEE Trans. Pattern Anal. Mach. Intell. 25 (8) (2003) 1009–1014.

[2] A.K. Jain, L. Hong, S. Pankanti, R. Bolle, An identity-authentication system using fingerprints, Proc. IEEE 85 (9) (1997) 1365–1388.

[3] A.K. Jain, L. Hong, R. Bolle, On-line fingerprint verification, IEEE Trans. Pattern Anal. Mach. Intell. 19 (3) (1997) 302–313.

[4] T. Hatano, T. Adachi, S. Shigematsu, H. Mirimora, S. Onishi, Y. Okasaki, H. Kyuragi, A fingerprint verification using the differential matching rate, in: Proceedings of the International Conference on Pattern Recognition, vol. 3, 2002, pp. 799–802.

[5] C. Wilson, C. Watson, E. Paek, Effect of resolution and image quality on combined optical and neural network fingerprint matching, Pattern Recognition 33 (2) (2000) 317–331.

[6] A. Jain, S. Prabhakar, L. Hong, S. Pankanti, FingerCode: a filterBank for fingerprint representation and matching, in: Proceedings of IEEE Computer Society Conference on Computer Vision and Pattern Recognition (CVPR), vol. 2, 1999, pp. 187–193.

[7] L. Sha, F. Zhao, X. Tang, Improved FingerCode for filterbank-based fingerprint matching, IEE Proc. Visual Image Signal Process. 145 (3) (1998) 160–166.

[8] A.J. Willis, L. Myers, A cost-effective fingerprint recognition system for use with low-quality prints and damaged fingertips, Pattern Recognition 34 (2) (2001) 255–270.

[9] M. Tico, P. Kuosmanen, J. Saarinen, Wavelet domain features fingerprint recognition, Electron. Lett. 1 (2001) 21–22.

[10] Y. Hamamoto, A gabor filter-based method for fingerprint identification, in: L.C. Jain, U. Halici, I. Hayashi, S.B. Lee (Eds.), Intelligent Biometric Techniques in Fingerprint & Face Recognition, CRC Press, Boca Raton, FL, 1999.

[11] A.K. Jain, A. Ross, S. Prabhakar, A hybrid fingerprint matching using minutiae and texture features, in: Proceedings of the International Conference on Image Processing (ICIP), 2001, pp. 282–285.

[12] K.C. Chan, Y.S. Moon, P.S. Cheng, Fast fingerprint verification using subregions of fingerprint images, IEEE Trans. Circuits Syst. Video Technol. 14 (1) (2004) 95–101.

[13] N.K. Ratha, K. Karu, S. Chen, A.K. Jain, A real-time matching system for large fingerprint databases, IEEE Trans. Pattern Anal. Mach. Intell. 18 (8) (1996) 799–813.

[14] D.H. Ballard, Generalized hough transform to detect arbitrary patterns, IEEE Trans. Pattern Anal. Mach. Intell. 3 (2) (1981) 111–122.

[15] Z.M. Kovacs-Vajna, A fingerprint verification system based on triangular matching and dynamic time warping, IEEE Trans. Pattern Anal. Mach. Intell. 22 (11) (2000) 1266–1276.

[16] X. Jiang, W.Y. Yau, Fingerprint minutiae matching based on the local and global structures, in: 15th Proceedings of the International Conference on Pattern Recognition, vol. 2, 2000, pp. 1042–1045.

[17] A.M. Bazen, S.H. Gerez, An intrinsic coordinate system for fingerprint matching, in: Third International Conference on Audio and Video-based Biometric Person Authentifcation, Halmstad, Sweden, 2001, pp. 198–204.

[18] D. Maltoni, D. Maio, A.K. Jain, S. Prabhakar, Handbook of Fingerprint Recognition, Springer, New York, 2003.

[19] D. Maio, D. Maltoni, Direct gray-scale minutiae detection in fingerprints, IEEE Trans. Pattern Anal. Mach. Intell. 19 (1) (1997) 27–40.

[20] A.M. Bazen, S.H. Gerez, Directional field computation for fingerprints based on the principal component analysis of local gradients, in: Proceedings of ProRISC2000, 11th Annual Workshop on Circuits, Systems and Signal Processing, Veldhoven, The Netherlands, 2000.

[21] F. Benhammadi, H. Hentous, K. Beghdad Bey, M. Aissani, Fingerprint matching using oriented-dependent minutiae, in: IASTED VIIP, Acta Press, 2005, pp. 33–38, ISBN 0-88986-528-0.

[22] D. Maio, D. Maltoni, R. Cappelli, J.L. Wayman, A.K. Jain, FVC2002: second fingerprint verification competition, 16th International Conference on Pattern Recognition, 2002, pp. 30811–30814.

[23] D. Maio, L. Nanni, An efficient fingerprint verification system using integrated gabor filters and Parzen window classifier, Neurocomputing 68 (2005) 208–216.

About the Author—FARID BENHAMMADI holds a diploma in Engineer degree in Computer Science. In 1999, he received the Ph.D. degree in Artificial Intelligence from Angers University, France. Cuurently he is an assistant professor in the area of logic programming, Artificial Intelligence, pattern recognition and UML.

About the Author—MOHAMMED NABIL AMIROUCHE holds a diploma in Engineer degree in Computer Science. In 2005 he received the Master's degree in Industrial Computer Science from M. Polytechnic school. Currently he is an assitant professor in the area of computer science.

About the Author—HAMID HENTOUS holds a diploma in Engineer degree in Computer Science. He received the Ph.D. degree in computer integrated manufacturing from INSA de LYON France in 1999. Currently he is an assistant professor in the area of scheduling and graph theory.

About the Author—KADDA BEY BEGHDAD holds a diploma in Engineer degree in Computer Science. In 2003 he received the Master's degree in Industrial Computer Science from Polytechnic school. Currently he is an assistant professor in the area of language theory and images processing.

About the Author—MOHAMED AISSANI holds a diploma in Engineer degree in Computer Science. He received the Master's degree in Artificial Intelligence from USTHB University, Algeria in the year 2000. Currently he is an assistant professor in the area of Artificial Intelligence and neuronal networks.